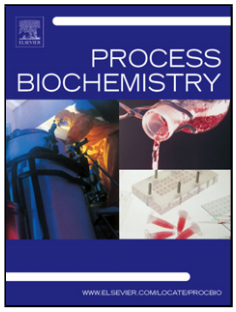

Title: Cytotoxic effect of Green synthesized silver nanoparticles using *Melia azedarach* against *in vitro* HeLa cell lines and lymphoma mice model

Authors: Raman Sukirtha, Kandula Manasa Priyanka, Jacob Joe Antony, Soundararajan Kamalakkannan, Thangam Ramar, Gunasekaran Palani, Muthukalingan Krishnan, Shanmugam Achiraman

PII: S1359-5113(11)00400-4
DOI: doi:10.1016/j.procbio.2011.11.003
Reference: PRBI 9392

To appear in: *Process Biochemistry*

Received date: 25-9-2011
Revised date: 2-11-2011
Accepted date: 3-11-2011

Please cite this article as: Sukirtha R, Priyanka KM, Antony JJ, Kamalakkannan S, Ramar T, Palani G, Krishnan M, Achiraman S, Cytotoxic effect of Green synthesized silver nanoparticles using *Melia azedarach* against *in vitro* HeLa cell lines and lymphoma mice model, *Process Biochemistry* (2010), doi:10.1016/j.procbio.2011.11.003

Highlights

- Fast synthesis of *M. azedarach* derived stable AgNPs at 95°C
- Cytotoxicity comparison of AgNPs with 5- FU against HeLa cell lines.
- *In vivo* cytotoxicity against Dalton's ascites lymphoma

Cytotoxic effect of Green synthesized silver nanoparticles using *Melia azedarach* against *in vitro* HeLa cell lines and lymphoma mice model

Raman Sukirtha [a], Kandula Manasa Priyanka [a], Jacob Joe Antony [a], Soundararajan Kamalakkannan [a], Thangam Ramar [b], Gunasekaran Palani [b], Muthukalingan Krishnan [a], Shanmugam Achiraman [a*]

[a] Department of Environmental Biotechnology, School of Environmental Sciences, Bharathidasan University, Tiruchirappalli-620 024, India.

[b] Department of Virology, King Institute of Preventive Medicine and Research, Guindy, Chennai-600 032, India.

Correspondence: Dr. S. Achiraman, Info chemicals and Nano oncology Lab, Department of Environmental Biotechnology, School of Environmental Sciences, Bharathidasan University, Tiruchirappalli- 620 024, Tamilnadu, India.

E-mail: achiramans@gmail.com; Phone: 00-91-431-2407088; Fax: 00-91-431-2407045

ABSTRACT

This communication explains the biosynthesis of stable silver nanoparticles (AgNPs) from *Melia azedarach* and its cytotoxicity against *in vitro* HeLa cells and *in vivo* Dalton's ascites Lymphoma (DAL) mice model. The AgNPs synthesis was determined by UV- visible spectrum and it was further characterized by Scanning Electron Microscopy (SEM), Dynamic light Scattering (DLS) and X-Ray Diffraction (XRD) analysis. Zeta potential analysis revealed stable AgNPs with -24.9 mV. UV visible spectrum indicated an absorption peak at 436 nm which reflects its specific Surface Plasmon Resonance (SPR). Biosynthesized AgNPs were predominantly cubical and spherical with an average particle size of 78 nm approximately as observed through SEM and DLS analysis respectively. Cytotoxicity of biosynthesized AgNPs against *in vitro* Human epithelial carcinoma cell line (HeLa) showed a dose-response activity. Lethal dose (LD_{50}) value was found to be 300 µg/ mL of AgNPs against HeLa cell line. Cytotoxicity against normal continuous cell line human breast lactating, donor 100 (HBL 100) was found only in increased concentration of both AgNPs and 5- FU. In addition, *in vivo* DAL mice model showed significant increase in life span, induction of apoptosis was evidenced by acridine orange and ethidium bromide (AO and EB) staining.

Keywords: *Melia azedarach*, AgNPs, DLS, XRD, HeLa, DAL.

1. Introduction

Dependence of human life on nanotechnology was emerged naturally from ayurveda, a 5000-year-old system of Indian medicine. Though the modern science has started exploring the term 'Nano' in 21st century, ayurvedic medicinal systems used noble metals such as gold, silver etc. in nanoform as basmas for various medical applications [1]. Since nanoparticles (NPs) are more biocompatible than the conventional therapeutics, they are exploited for drug encapsulation and delivery [2]. It has been stressed over the years that size reduction of NPs play an important role in improving their bio availability as well as compatibility for therapeutical applications in diseases like cancer [3]. Silver nanoparticles (AgNPs) have a great potential in cancer management because it selectively involved disruption of the mitochondrial respiratory chain by AgNPs leading to production of ROS and interruption of ATP synthesis, which in turn cause DNA damage [4, 5].

With Food and Drug Administration (FDA) approval, AgNPs were known to be effective against bacterial and viral mediated diseases and possess a huge potential in treating various diseases like retinal neovascularization, cancer, hepatitis B, acquired human immunodeficiency (HIV), diabetes, etc in the near future [6]. To date, several methods were employed for the synthesis of AgNPs modes ranging from chemical procedures [7], radiation [8], electrochemical [9] and photochemical methods [10]. Very recently, biological synthesis of nanoparticles is in application for its ecofriendly mode of synthesis with passable biomedical applications [11, 12].

In pursuit of novel eco-friendly methods, plant possessing thousand of biologically active compounds may exploited as key resource for the green synthesis of nanoparticles [13] and serve as an alternate to the existing chemical, physical and even microbial methods [14]. Studies

conducted by Gardea–Torresdey et al. [12] and Shankar et al. [15] on the synthesis of gold nanoparticles by living plants, has described their potential biomedical applications. Very recently, it has been reported that plants rich in tannic acid have a great potential to synthesize AgNPs which also confers stability to the nanoparticles [16]. The rationale behind the use of plants for the synthesis of AgNPs is not only that it is simple, faster and easy but the synthesized particles were also stable, reliable and cost effective than other conventional methods [17].

Melia azedarach Linn (Meliaceae; Neem) is an indigenous plant to Indian subcontinent possessing several medicinal properties and has been in use for centuries. Traditionally, the plant possess several therapeutic properties such as anti-helminthic [18], anti-fungal [19], anti-malarial activity [20], anti-bacterial and anti-oxidant [21] properties. Its leaf extract possess antiviral [22] and anti-infertility activities [23]. In a recent study, the cytotoxic activity of *M. azedarach* was reported against human lung adenocarcinoma epithelial cell lines [24]. With these evidences, here we investigated the green synthesis of AgNPs using aqueous extract obtained from leaf of *M. azedarach* and its cytotoxicity against *in vitro* HeLa, HBL 100 cell lines and *in vivo* DAL cell line in mice model.

2. Materials and methods

2.1. Preparation of leaf aqueous extract

Authenticated *M. azedarach* L. was collected from the local surroundings of Tiruchirappalli with the help of a field botanist of Bharathidasan University, Tiruchirappalli, India. Fresh leaves were used for the extraction of the active components. The leaves were shade dried for 2 to 3 weeks at room temperature and then powdered. Briefly, 5 g of leaf powder was weighed and mixed in 100 mL of millipore water. This mixture was boiled in water bath at 60 °C

for 10- 20 min. After cooling to room temperature, the mixture was filtered by using muslin filter cloth (0.2 μm) and used for the study.

2.1.1. Green Synthesis of AgNPs

Biological synthesis of AgNPs was carried out following Song et al [25] method. Typically, 10 mL of aqueous extract was added to 190 mL of 1 mM aqueous silver nitrate solution for the reduction of Ag^{+} ions. The effects of temperature on the synthesis rate of the AgNPs were studied by carrying out the reaction at 30– 95 °C for 10 min. The AgNPs solution, thus obtained was purified by repeating the centrifugation thrice at 7,000 rpm for 20 min at 4 °C followed by redispersion of the pellet in Milli-Q water.

2.1.2. Characterization of AgNPs

UV–visible spectra were recorded as a function of the reaction time on a UV- 1601 PC spectrophotometer (Shimadzu, Japan) operated at a resolution of 1 nm. The purified AgNPs were examined for the presence of biomolecules using FTIR analysis. The spectrum obtained from the dried sample was recorded on FTIR spectrum RX-1 instrument (Perkin- Elmer), USA in the diffuse reflectance mode at a resolution of 4 cm^{-1} in KBr pellets. Crystalline AgNPs were determined by X-ray diffraction analysis. Briefly, the biosynthesized AgNPs were laid onto the glass substrates on a Phillips PW 1830 instrument operating at a voltage of 40 kV and a current of 30 mA with Cu$K\alpha$ radiation. The shape of the freeze dried AgNPs was analyzed by SEM (SEM- Hitachi model- S 3000H). The particle size distribution of AgNPs was evaluated using dynamic light scattering (DLS) measurements and zeta potential analysis were conducted with a Malvern Zetasizer Nanoseries compact scattering spectrometer (Malvern Instruments Ltd,

Malvern, UK). The AgNPs were dissolved in physiological saline for zeta potential analysis. Data obtained were analyzed using Zetasizer software.

2.2. In vitro cytotoxicity of biosynthesized AgNPs

HeLa and HBL 100 cells were purchased from National Centre for Cell Science (NCCS), Pune and maintained in Eagle's Minimum essential medium and McCoys 5a medium respectively, supplemented with calf serum (10%) and non-essential amino acids. Cells were cultured at 37 °C in a humidified atmosphere containing 5 % CO_2 in air. Both HeLa and HBL 100 cells were cultured and seeded into 96 well plates approximately as 1 x 10^4 cells in each plate and incubated for 48 hrs. Both HeLa and HBL 100 cells were treated with a series of 100 µg/ mL to 1000 µg/ mL concentration of biosynthesized AgNPs along with cell control and AgNPs control (drug control). At the same time we have compared both the cells with known anticancer agent, 5- Fluoro Uracil (5-FU) in a stock concentration of 100 mM. Series concentration 100- 1000 µM/ mM of 5- FU were treated in both cells. These treated plates were incubated for 48- 72 hrs for cytotoxic analysis. Then these plates were subjected for MTT assay. MTT (3-(4, 5-Dimethylthiazol-2-yl)-2, 5-diphenyltetrazolium bromide, a yellow tetrazole) was prepared in 5 mg/mL concentration. 100 µl of MTT was added in each well and incubated for 4 hrs. Purple color formazone crystals formed, were then dissolved with 100 µl of Di-methyl sulphoxide (DMSO). These crystals were observed at 620 nm in a Multi well ELISA plate reader. OD value was subjected to sort out percentage of viability by using the following formula,

$$\text{Percentage of viability} = \frac{\text{OD value of experimental samples (AgNPs)}}{\text{OD value of experimental control (untreated)}} \times 100$$

2.3. Investigation of antitumor activity of aqueous and biosynthesized AgNPs

DAL cells were obtained under the courtesy of Amala Cancer Research Center, Thrissur, Kerala, India. They were maintained by intraperitoneal inoculation of $1x10^6$ cells per mouse (Swiss albino male with 30 g body weight) in accordance with the guidelines of animal care by the Institutional Animal Ethical Committee (IAEC), Bharathidasan University, India.

2.3.1. Experimental groups

Mice were divided into six groups containing six mice per group (n=6). Group I remained neither untreated nor injected with DAL cells and represented as normal. From group II to VI all mice were injected with DAL cells (10^6 cells per mouse) by intra-peritoneal (IP) route and this was taken as day zero. Group II served as tumor control and did not receive plant extract or AgNPs. After 24 hrs of tumor induction animals in group III received 50 mg per Kg BW of aqueous extract of *M. azedarach* through intraperitoneal administration. Alike, mice from group IV to VI received doses of AgNPs containing 300, 500 and 700 µg per Kg BW respectively. At the end of the experiment, 2 to 3 mL of sterile PBS was injected into the peritoneal cavity of the experimental mice and the ascitic fluid containing the tumor cells were withdrawn. From day zero life span of all the experimental groups was observed. The percentage of viable and dead cells along with the degree of cytotoxicity was determined by acridine orange staining.

2.3.2. Acridine Orange (AO) and Ethidium Bromide (EB) staining

Tumor cells collected were washed with phosphate buffered saline PBS (pH- 7.2) and stained by adding 1 mL of AO and EB mix (100 mg per mL AO and 100 mg per mL EB in PBS). After 2 min incubation, cells were washed twice with PBS (5 min each) and visualized under fluorescence microscope (Olympus, Japan) at 400 X magnification with excitation filter 480 nm. The percentage of apoptotic cells were determined by,

Calculation:

$$\text{Percentage of apoptotic cells} = \frac{\text{Total number of apoptotic cells}}{\text{Total number of normal and apoptotic cells}} \times 100$$

2.4. Statistical analysis

The statistical analysis was done among the experimental groups with control and normal groups using SPSS software Version 16 (SPSS Inc Chicago, IL, USA). The One-way ANOVA was done for expressing experimental significance of the present study. Statistical significance was accepted at a level of $p < 0.05$.

3. Results and Discussion

3.1. Confirmation of biosynthesized AgNPs

Taking advantage of the rich tannic acid content of *M. azedarach*, which is known to mediate the formation of silver nanoparticles [15], the present study was aimed to synthesize the same from aqueous extract of *M. azedarach* leaves and its cytotoxicity was determined against *in vitro* cancer cell lines (HeLa, HBL 100) and *in vivo* lymphoma mice model. Evaluating the synthesis at different temperatures, intensity of yellowish brown color developed was elevated at

95 °C, compared to other temperatures such as 30 °C, 60 °C and 90 °C (Fig. 1). This colour change determines the synthesis of AgNPs from aqueous extract of *M. azedarach* [26]. In the present study, supporting the color change spectral band peak of corresponding temperatures confirmed the maximum synthesis at 95 °C (Fig. 2). Our results were in accordance with earlier results of Shaligram et al. [27] emphasizing Surface Plasmon Resonance (SPR) peak of metal nanoparticles. The formation of AgNPs [28, 29] was mediated by the active principles present in aqueous extract of *M. azedarach.* There are evidences which states that tannic acid hydrolyses into glucose and gallic acid under mild acidic or basic conditions and in turn gallic acid formed rapidly reduces silver nitrate into AgNPs [30]. Strictly pursuing Sivaraman et al. [16] the results suggested in the present study for biosynthesis of AgNPs could have occurred in a similar fashion.

AgNPs characterization and its associated molecules

Fig. 3. showed the FTIR spectra of aqueous extract of air-dried leaves of *M. azedarach* and purified AgNPs of various temperatures. The FTIR peaks determined the bonds in relevance to alcoholic O-H stretching (3433 cm^{-1}), aldehyde C-H stretching (2830 cm^{-1}), amine N-H stretching (3409 cm^{-1}) and bending (1631 cm^{-1}), primary amines (665 cm^{-1}) and germinal methyl bending (1353 cm^{-1}). The band at 1631 cm^{-1} suggested the presence of amide group, raised by the carbonyl stretch of proteins. These results indicated that the carbonyl group of proteins adsorbed strongly to metals, indicating that proteins could have also formed a layer along with the bio-organics, securing nanoparticles. This implicit and proved that the polyphenolics like tannic acid conferred the free energy to reduce the silver ions to AgNPs. These results were similar to the reports of Dubey et al. [31]

XRD patterns of nanoparticles exhibit several size dependent features leading to peak position, heights and widths. In the present study sharp peaks were observed other than silver region (Fig. 4). These might have resulted from the bio-organic compounds in the *M. azedarach*. The obtained results were supported by the results stated by Shankar et al. [15]. The number of Braggs reflections obtained in the current study (200), (111), (311) corresponds to the diffraction facets of silver and indexed for the presence of crystalline silver nanoparticles. These interpretations were also similar to the results of Dubey et al. [31]

The SEM images showed the presence of cubes and spherical structures of AgNPs (Fig. 5a). These results were in accordance with results of Kalimuthu et al. [32]. DLS analysis showed the size distribution of particles with maximum intensity at 78 nm (Fig. 5b). Our findings were similar to the report of Haefeli et al. [33]. In practice, dispersion is stable if the zeta potential is higher than 30 mV or lower than -30 mV. The zeta potential of the particles, however, strongly depends on the pH and the electrolyte concentration of the dispersion [34]. Supporting the above statement AgNPs dispersed in physiological saline was highly stable with zeta potential value – 24.9 mV (Fig. 5c).

3.2. In vitro cytotoxicity of biosynthesized AgNPs

Despite the widespread use of synthetic AgNPs, there are only a few studies to determine the cytotoxic effects of biologically synthesized AgNPs, particularly in the context of apoptosis. MTT assay was used to assess the effect of AgNPs on proliferation of HeLa cells and normal HBL100 cells. This is the first study to evaluate *M. azedarach* derived AgNPs cytotoxicity against cancer cell lines. Thus we hypothesize that cell killing could be the possible mechanism induced by the cytotoxic effect of biosynthesized AgNPs.

The dose dependent cytotoxicity was observed in AgNPs treated HeLa cells and the increase in concentration of AgNPs showed increased cytotoxicity in HeLa cells. Fifty percent of cell death which determines the LD_{50} value of biosynthesized AgNPs against HeLa cells holds at 300 µg/ mL concentration (Fig. 6a). Similar report of cytotoxicity was discussed by Sriram et al. [35] and Safaepour et al. [36]. The cytotoxic effect was compared with the standard anticancer drug 5- FU against HeLa cells (Fig. 6b) and their LC_{50} value was observed with 600 µg/ 100 mM. Similarly cytotoxicity of chemically synthesized AgNPs was reported against HeLa cells by Miura and Shinohara [37]. Effect of biosynthesized AgNPs and 5- FU on growth of normal cell line (HBL 100) did not exhibit significant cytotoxicity at their lower concentration and its increases with its increased concentration, at 750 µg/ mL and 1000 µg/ 100 mM respectively (Fig. 6c & d). A large number of *in vitro* studies indicate that AgNPs are toxic to the mammalian cells [38]. Interestingly, some studies have shown that AgNPs has the potential to intervene genes associated with cell cycle progression, also induce DNA damage and apoptosis in cancer cells [39]. Indeed, our results provide conclusive evidence for cytotoxic effect of AgNPs on cancer cell lines rather than normal cell lines.

In vivo cytotoxicity of biosynthesized AgNPs

In addition to these results, *in vivo* study of biosynthesized AgNPs revealed an increased life span in a dose dependent manner, compared to the induced and other experimental groups (Fig. 7). To investigate, the mode of cell death either by apoptosis or from necrotic cell death, AO and EB staining was employed. In Fig. 8, green fluorescence emission was observed in untreated tumor cells (Gp2) due to the permeablization of AO, a cytoplasmic stain which specifically stains the live cells. AgNPs treated DAL cells exhibited reddish orange fluorescence

due to their loss in membrane integrity [40]. In addition, nuclear condensation, membrane blebbing, apoptotic bodies and cytoplasmic vacuoles were observed in DAL cells treated with 700 µg/ kg BW AgNPs than the other experimental groups. Thus percentage of apoptotic cells was statistically significant in AgNPs treated DAL cells and increased proportionately with its varying concentration. Comparatively less percentage of apoptotic cells were noticed in aqueous extract treated DAL tumor cells.

4. Conclusion

To conclude, the present study documented the first ever synthesis, characterization and cytotoxicity of biosynthesized AgNPs from *M. azedarach* against *in vitro* and *in vivo* models. Collectively, our data suggests that AgNPs possess superior cytotoxic activity compared to the *M. azedarach* aqueous extract. With little uncovered mechanism in the current study, there is a wide scope for detailed investigation in the future for the application of AgNPs in cancer therapy.

Acknowledgements

The authors thank Bharathidasan University, Tiruchirappalli, Tamilnadu for the University Research Fellowship. We also extend our acknowledgement to University Grant Commission, University Grant Commission- Non Special Assistance Program, Department of Science and Technology Fast Track Scheme, Department of Science and Technology-Nano Mission, Council for Scientific and Industrial Research, Government of India for their financial assistance.

References

[1] Symposium on Ayurveda and Modern Biology at Arya Vaidya Chikitsalayam & Research Institute (AVC), Coimbatore, Tamilnadu; 29 July 2009.

[2] Wang X, Yang L, Chen Z, Shin DM. Application of Nanotechnology in Cancer Therapy and Imaging. CA Cancer J Clin 2008;58:97-110.

[3] Kim JS, Kuk E, Yu KN, et al. Antimicrobial effects of silver nanoparticles. Nanomedicine 2007;3:95-101.

[4] AshaRani PV, Grace Low Kah Mun, Manoor Prakash Hande, Suresh Valiyaveettil. Cytotoxicity and Genotoxicity of Silver Nanoparticles in Human Cells 2009;ACS Nano;3:279-290.

[5] Morones, JR, Elechiguerra, LJ, Camacho A, Holt K, Kouri BJ, Ramirez TJ, Yocaman JM. The bactericidal effect of silver nanoparticles. Nanotechnology 2005;16:2346- 2353

[6] Bhattacharya R, Mukherjee P. Biological properties of "naked" metal nanoparticles. Adv Drug Delivery Rev 2008;60:1289-1306.

[7] Hu R, Yong KT, Roy I, et al. Metallic nanostructures as localized plasmon resonance enhanced scattering probes for multiplex dark field targeted imaging of cancer cells. J Phys Chem C Nanomater Interfaces 2009;113:2676–2684.

[8] Dimitrijevic NM, Bartels DM, Jonah CD, Takahashi K, Rajh T. Radiolytically Induced Formation and Optical Absorption Spectra of Colloidal Silver Nanoparticles in Supercritical Ethane. J Phys Chem B 2001;105:954–959.

[9] Yin B, Ma H, Wang S, Chen S. Electrochemical Synthesis of Silver Nanoparticles under Protection of Poly (N-vinylpyrrolidone). J Phys Chem B 2003;107:8898-8904.

[10] Callegari A, Tonti D, Chergui M. Photochemically Grown Silver Nanoparticles with Wavelength-Controlled Size and Shape. Nano Lett 2003;3:1565–1568.

[11] Naik RR, Stringer SJ, Agarwal G, Jones SE, Stone MO. Biomimetic synthesis and patterning of silver nanoparticles. Nat Mater 2002;1:169-172.

[12] Gardea-Torresdey JL, Parsons JG, Gomez E, et al. Formation and Growth of Au Nanoparticles inside Live Alfalfa Plants. Nano Lett 2002;2:397-401.

[13] Ahmad N, Sharma S, Alam MK, et al. Rapid synthesis of silver nanoparticles using dried medicinal plant of basil. Colloids Surf B 2010;81.

[14] Safaepour M, Shahverdi AR, Shahverdi HR, Khorramizadeh MR, Gohari A. Green Synthesis of Small Silver Nanoparticles Using Geraniol and Its Cytotoxicity against Fibrosarcoma-Wehi 164. Avicenna J Med Biotech 2009;1:111-115.

[15] Shankar SS, Ahmad A, Pasricha R, Sastry M. Bioreduction of chloroaurate ions by geranium leaves and its endophytic fungus yields gold nanoparticles of different shapes. J Mater Chem 2003;13:1822.

[16] Sivaraman SK, Elango I, Kumar S, Santhanam V. A green protocol for room temperature synthesis of silver nanoparticles in Seconds. Current Science 2009;97:1055-1059.

[17] Mohanpuria P, Rana NK, Yadav SK. Biosynthesis of nanoparticles: Technological concepts and future applications. J Nanopart Res 2008;10:507-517.

[18] Szewczuk VD, Mongelli ER, Pomilio AB. *In vitro* anthelmintic activity of *Melia azedarach* naturalized in Argentina. Phytother Res 2006;20:993-996.

[19] Jabeen K, Javaid A, Ahmad E, Athar M. Antifungal compounds from *Melia azedarach* leaves for management of *Ascochyta rabiei*, the cause of chickpea blight. Nat Prod Res 2010;1–13.

[20] Nathan SS, Savitha G, George DK, Narmadha A, Suganya L, Chung PG. Efficacy of *Melia azedarach* L. extract on the malarial vector *Anopheles stephensi* Liston (Diptera: Culicidae). Bioresour Technol 2006;97:1316–1323.

[21] Kaneria M, Baravalia Y, Vaghasiya Y, Chanda S. Determination of Antibacterial and Antioxidant Potential of Some Medicinal Plants from Saurashtra Region India. Indian J Pharm Sci 2009;71:406–412.

[22] Alche LLE, Fereka GA, Meob M, Cotoa CE, Maierb MS. An Antiviral Meliacarpin from Leaves of *Melia azedarach.* Z Naturforsch 2003;58:215-219.

[23] Mandal R, Dhaliwal PK. Antifertility effect of *Melia azedarach* Linn. (dharek) seed extract in female albino rats. Indian J Exp Biol 2007;45:853-860.

[24] Ntalli NG, Cottiglia F, Bueno CA, et al. Cytotoxic Tirucallane Triterpenoids from *Melia azedarach* Fruits. Molecules 2010;15:5866-5877.

[25] Song JY, Jang H-K, Kim BS. Biological synthesis of gold nanoparticles using Magnolia kobus and Diopyros kaki leaf extracts. Process Biochem 2009;44:1133–8.

[26] Elumalai EK, Prasad TNVKV, Hemachandran J, Therasa SV, Thirumalai T, David E. Extracellular synthesis of silver nanoparticles using leaves of *Euphorbia hirta* and their antibacterial activities. Journal of Pharmaceutical Sciences and Research 2010;2:549-554.

[27] Shaligram NS, Bule M, Bhambure R, Singhal RS, Singh SK, Szakacs G, et al. Biosynthesis of silver nanoparticles using aqueous extract from the compactin producing fungal strain. Process Biochem 2009;44:939–43.

[28] Raman Sukirtha, Muthukalingan Krishnan, Rajamanickam Ramachandran, Soundararajan Kamalakkannan, Palanivel Kokilavani, Devaraj Sankar Ganesh, Soundrapandian Kannan, Shanmugam Achiraman. *Areca catechu* Linn. Derived Silver Nanoparticles: A Novel Antitumor Agent against Dalton's Ascites Lymphoma. International Journal of Green Nanotechnology 2011;3:2–12.

[29] Tripathy A, Raichur AM, Chandrasekaran N, Prathna TC, Mukherjee A. Process variables in biomimetic synthesis of silver nanoparticles by aqueous extract of *Azadirachta indica* (Neem) leaves. J Nanopart Res 2010;12:237-246.

[30] Martınez-Castanon GA, Nino-Martinez N, Martinez-Gutierrez F, Martinez-Mendoza JR, Ruiz F. Synthesis and antibacterial activity of silver nanoparticles with different sizes. J Nanopart Res 2008;10:1343–1348.

[31] Shashi Prabha Dubey, Manu Lahtinen, Mika Sillanpaa. Tansy fruit mediated greener synthesis of silver and gold nanoparticles. Process Biochem 2010;45:1065–1071.

[32] Kalimuthu K, Babu RS, Venkataraman D, Bilal M, Gurunathan S. Biosynthesis of silver nanocrystals by *Bacillus licheniformis*. Colloids and Surf B 2008;65:150–3.

[33] Haefeli C, Franklin C, Hardy K. Plasmid- determined silver resistance in Pseudomonas stutzeri isolated from a silver mine. J. Bacteriol. 1984:158(1):389-392.

[34] Müller RH and Akkar A. Drug Nanocrystals of Poorly Soluble drugs. Encyclopedia of Nanoscience and Nanotechnology. American Scientific Publishers 2004;2:627 - 638.

[35] Muthu Irulappan Sriram, Selvaraj Barath Mani Kanth, Kalimuthu Kalishwaralal, Sangiliyandi Gurunathan. Antitumor activity of silver nanoparticles in Dalton's lymphoma ascites tumor model. Int J Nanomedicine 2010;5:753-762.

[36] Mona Safaepour, Ahmad Reza Shahverdi, Hamid Reza Shahverdi, Mohammad Reza Khorramizadeh, Ahmad Reza Gohari. Green Synthesis of Small Silver Nanoparticles Using Geraniol and Its Cytotoxicity against Fibrosarcoma-Wehi 164. Avicenna Journal of Medical Biotechnology 2009;1:111-115.

[37] Nobuhiko Miura and Yasushi Shinohara. Cytotoxic effect and apoptosis induction by silver nanoparticles in HeLa cells Biochemical and Biophysical Research Communications 2009;390: 733–737.

[38] Maqusood Ahamed, Mohamad S AlSalhi, Siddiqui MKJ. Silver nanoparticle applications and human health. Clinica Chemica Octa 2010;411; 841-1848.

[39] Pallab Sanpui, Arun Chattopadhyay, Siddhartha Sankar Ghosh. Induction of Apoptosis in Cancer Cells at Low Silver Nanoparticle Concentrations using Chitosan Nanocarrier. ACS Applied Materials and Interfaces 2011;3:218–228.

[40] Bhattacharyya SS, Mandal SK, Biswas R et al. *In vitro* Studies Demonstrate Anticancer Activity of an Alkaloid of the Plant *Gelsemium sempervirens*. Experimental Biology and Medicine 2008;233:1591-1601.

Figure Legends

Fig. 1: Color intensity of biosynthesized AgNPs at varying temperatures.

Fig. 2: UV spectral peak of AgNPs synthesized at different temperatures.

Fig. 3: Overlapped image of FTIR band peaks showing the oxidized biomolecules in the AgNPs synthesis. 1- FTIR peaks of aqueous plant extract; 2- Intense of FTIR band shift at 30 °C; 3- Intense of FTIR band shift at 60 °C; 4- Intense of FTIR band shift at 90 °C; 5- Intense of FTIR band shift at 95 °C;

Fig. 4: XRD pattern of AgNPs exhibiting the facets of crystalline Silver.

Fig. 5a: Topographical results of AgNPs confirming the cubical and spherical shaped particles from SEM analysis.

Fig. 5b: Size distribution of AgNPs with maximum intensity at 78 nm.

Fig. 5c Stable AgNPs with – 24.9 mV in Zeta potential analysis.

Fig. 6a: MTT assay results confirming the *in vitro* cytotoxicity of AgNPs against HeLa cell lines; DC- Drug control (AgNPs control) and CC- cell control.

Fig 6b: Cytotoxicity effect of 5- FU against HeLa cells; CC- cell control

Fig 6c: Effect of AgNPs on normal cell line (HBL 100) growth; CC- cell control.

Fig 6d: Effect of 5-FU on normal cell line (HBL 100) growth; DC- Drug control (AgNPs control) and CC- cell control.

Fig. 7: Graphical representation of life span depicting significant increase in AgNPs treated group than the control group; Gp- Group.

Fig. 8 Histogram representation of the percentage of apoptotic cells. Results are represented as a mean with bars showing mean ± SD; Gp- Group.

Fig. 1

Click here to download high resolution image

Fig. 2

Click here to download high resolution image

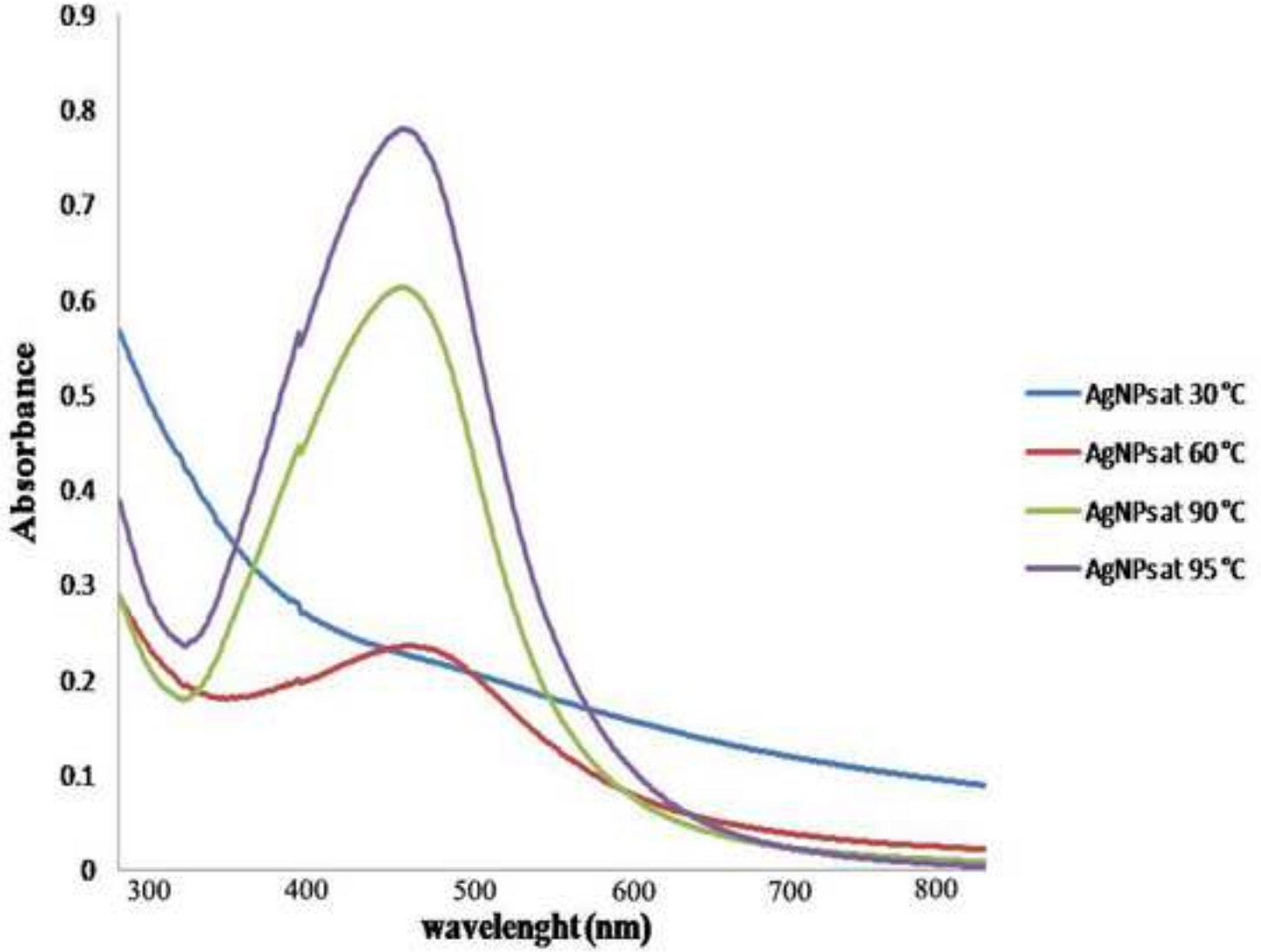

Fig. 3

Click here to download high resolution image

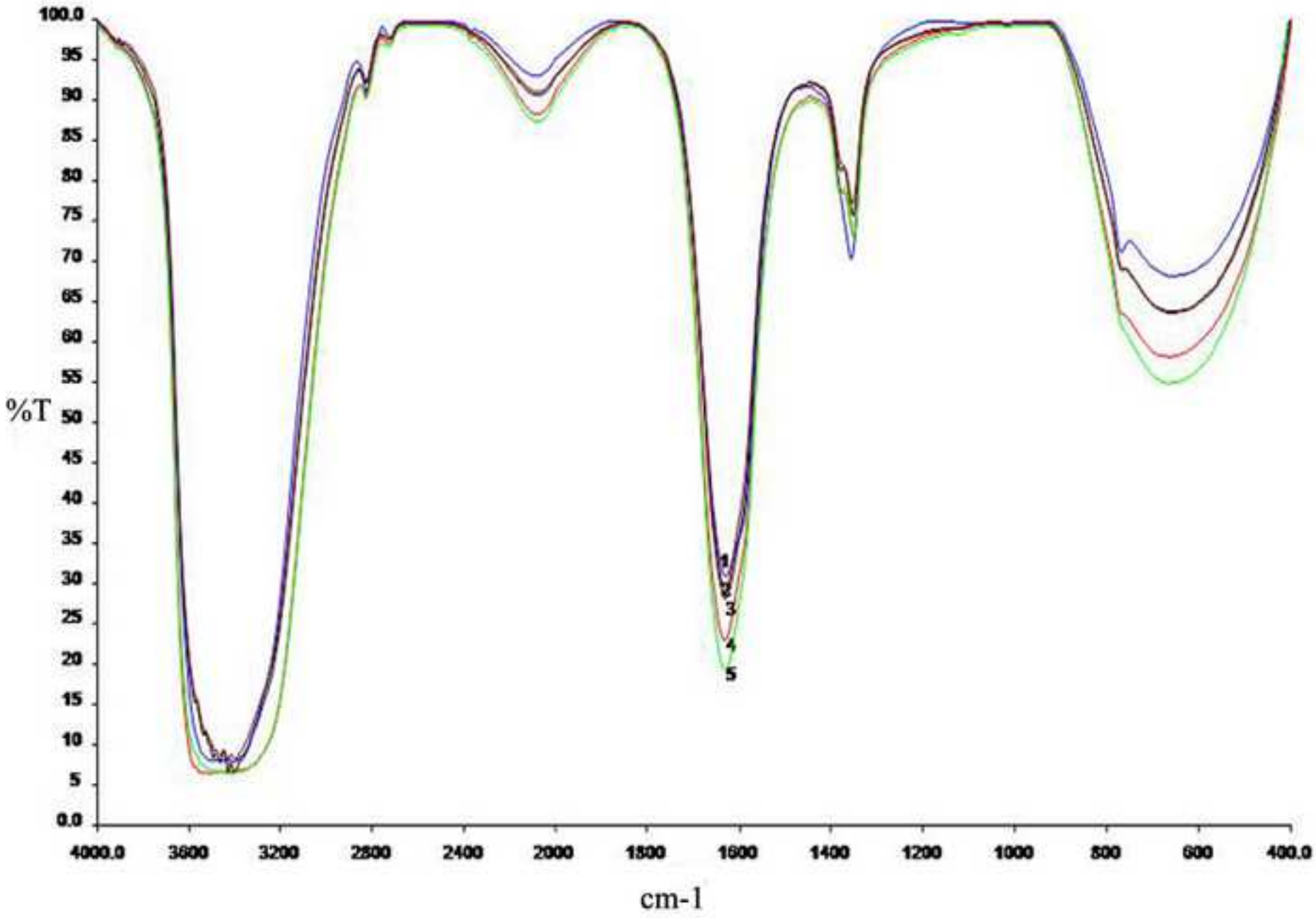

Fig. 4

Click here to download high resolution image

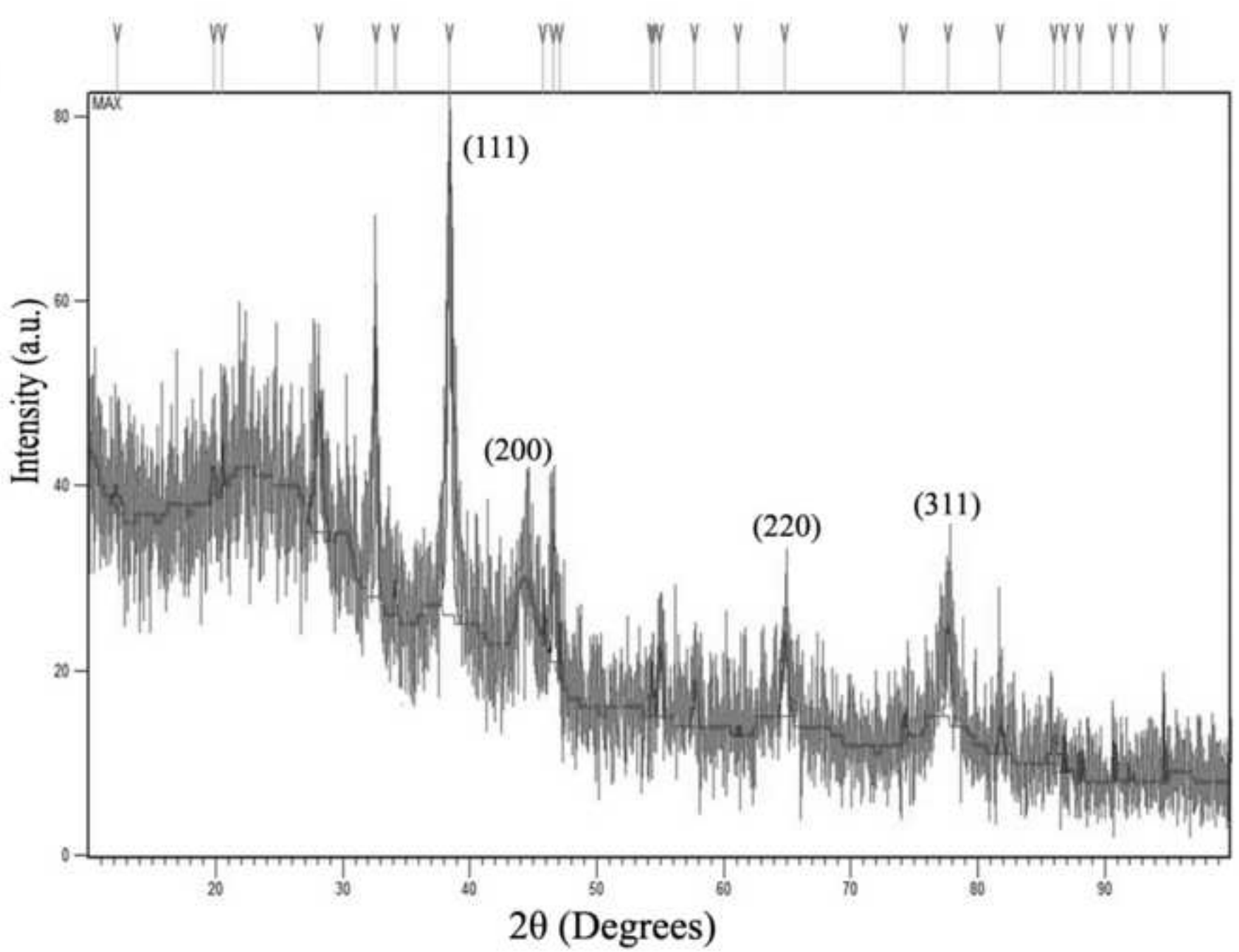

Fig. 5a

Click here to download high resolution image

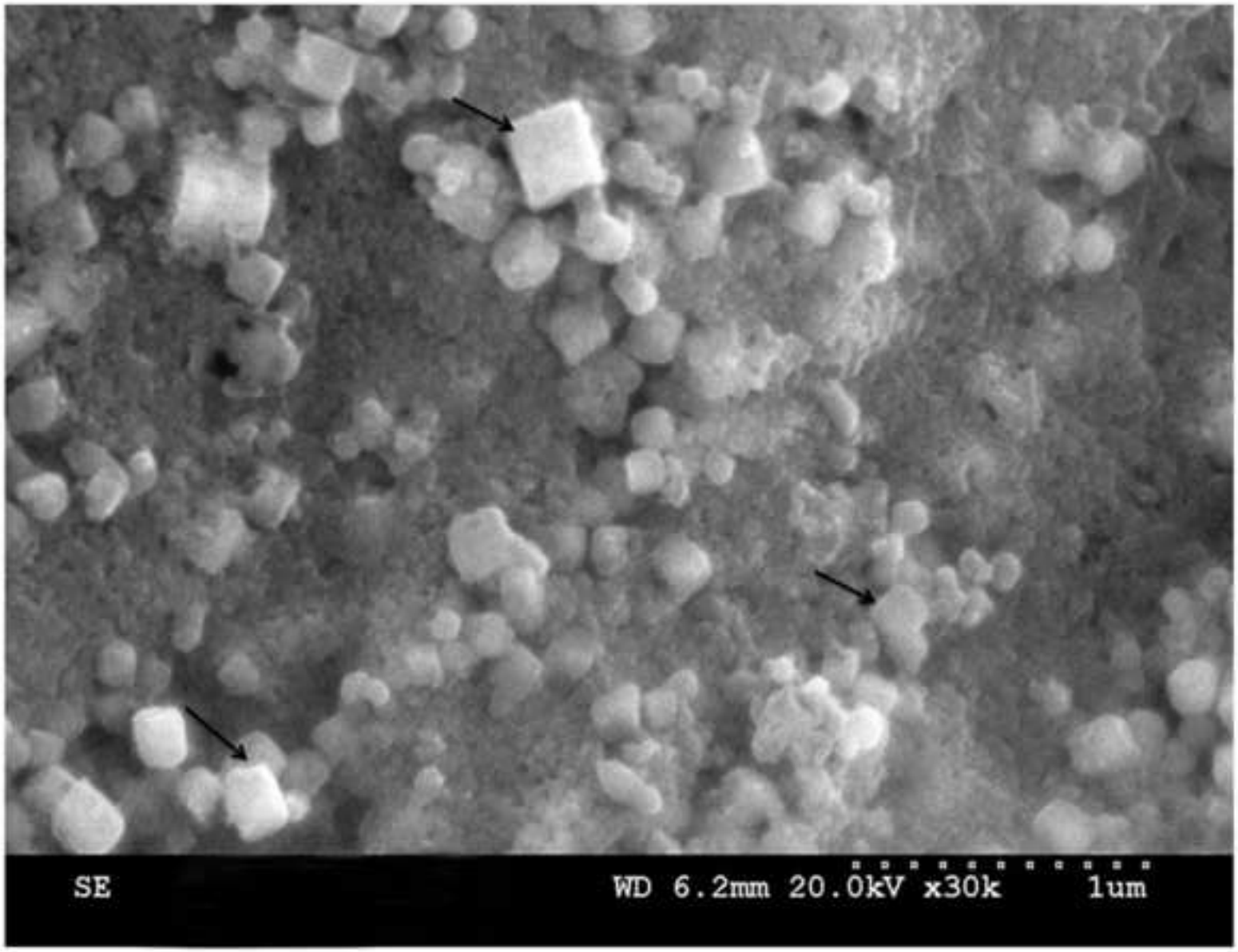

Fig. 5b
Click here to download high resolution image

Results

		Diam. (nm)	% Intensity	Width (nm)
Z-Average (d.nm): 78.19	Peak :	95.07	95.7	63.76
Result quality : Good				

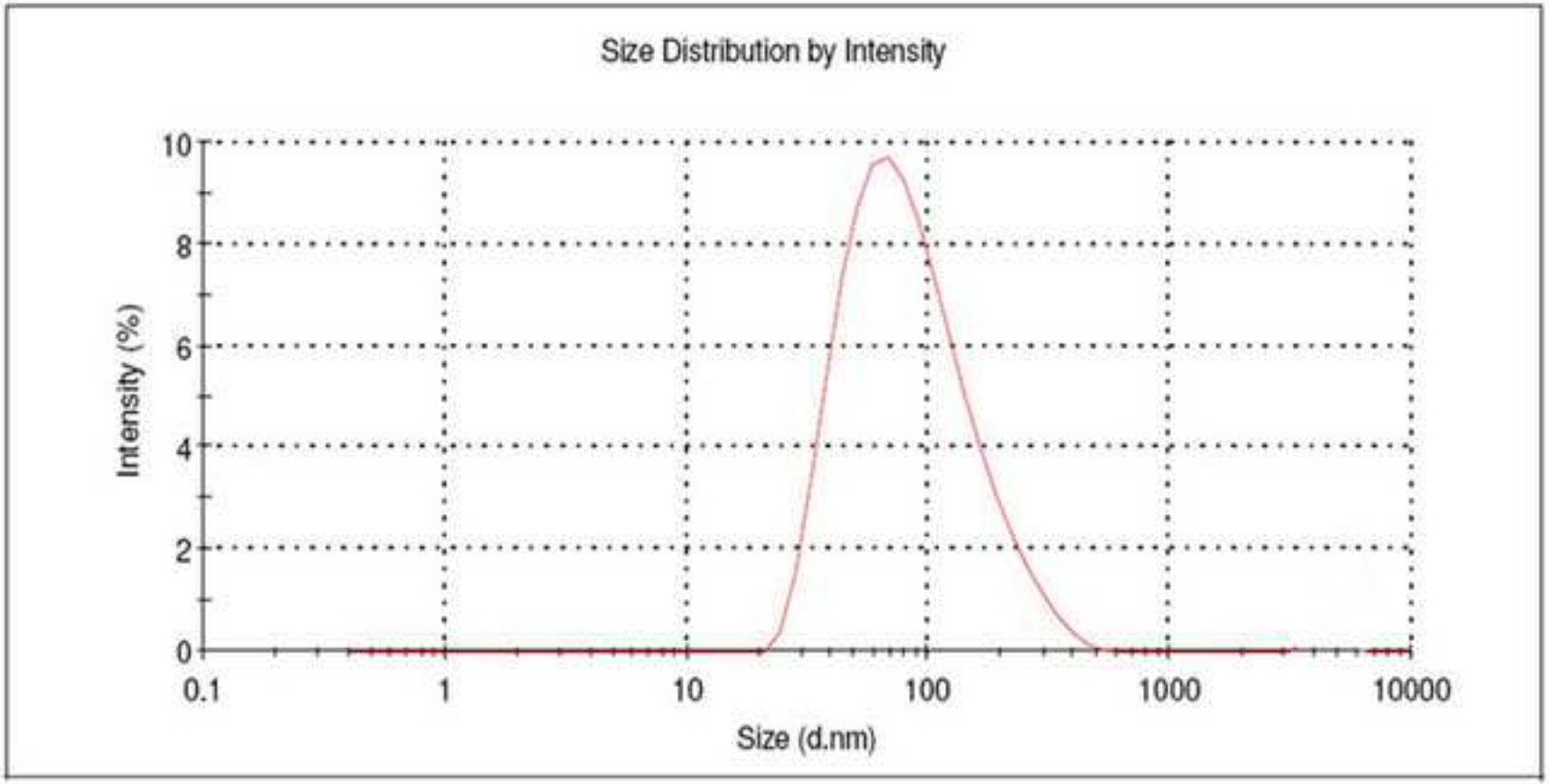

Fig. 5c
Click here to download high resolution image

Results

		Mean (mV)	Area (%)	Width (mV)
Zeta Potential (mV): -24.9	Peak 1:	-24.9	100.0	5.04
Zeta Deviation (mV): 5.04	Peak 2:	0.00	0.0	0.00
Conductivity (mS/cm): 2.48	Peak 3:	0.00	0.0	0.00

Result quality : Good

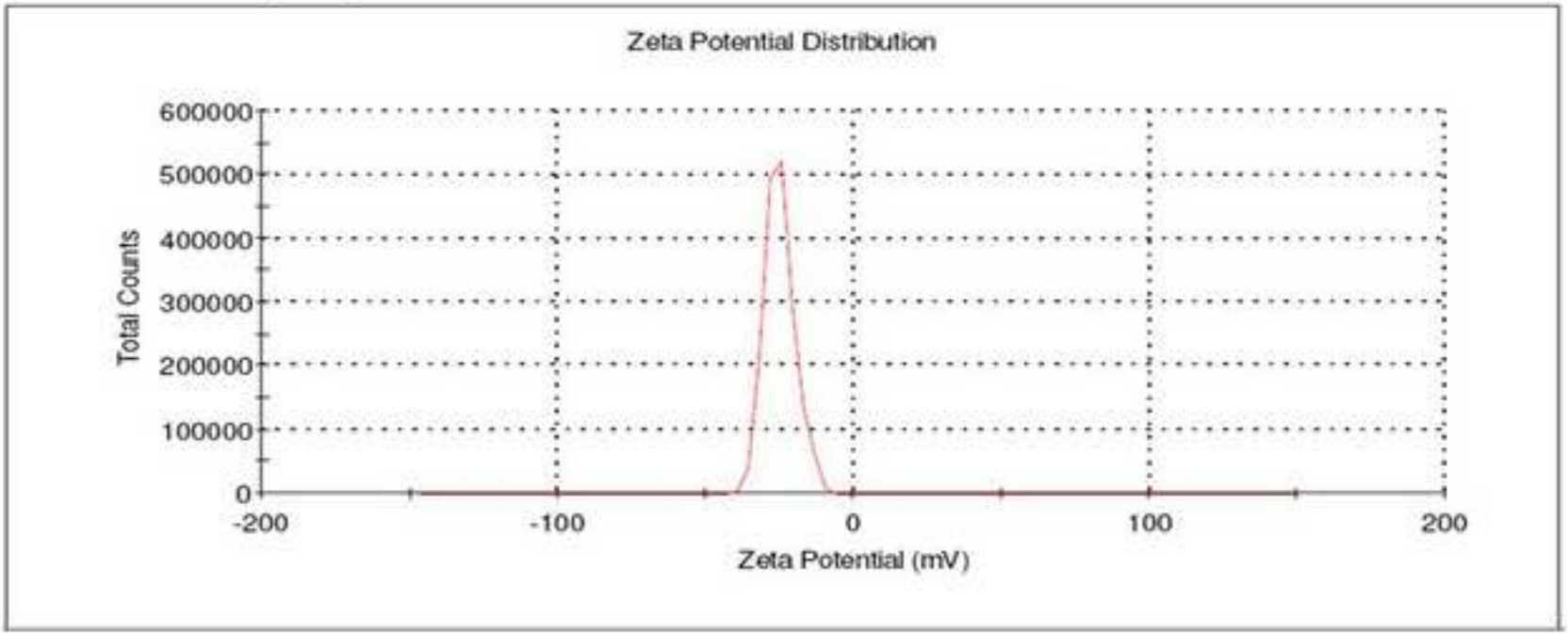

Fig. 6a

Click here to download high resolution image

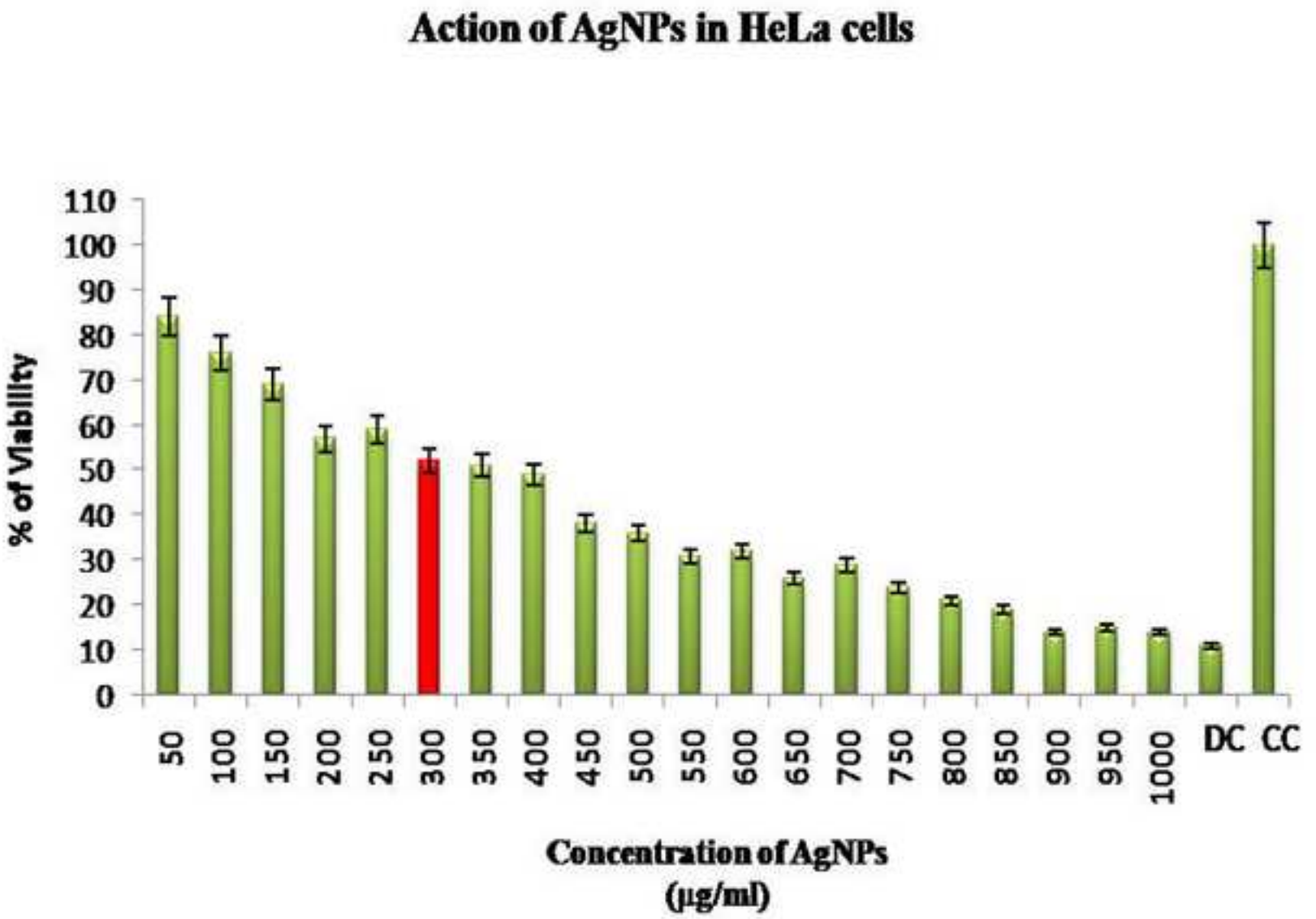

Fig. 6b

Click here to download high resolution image

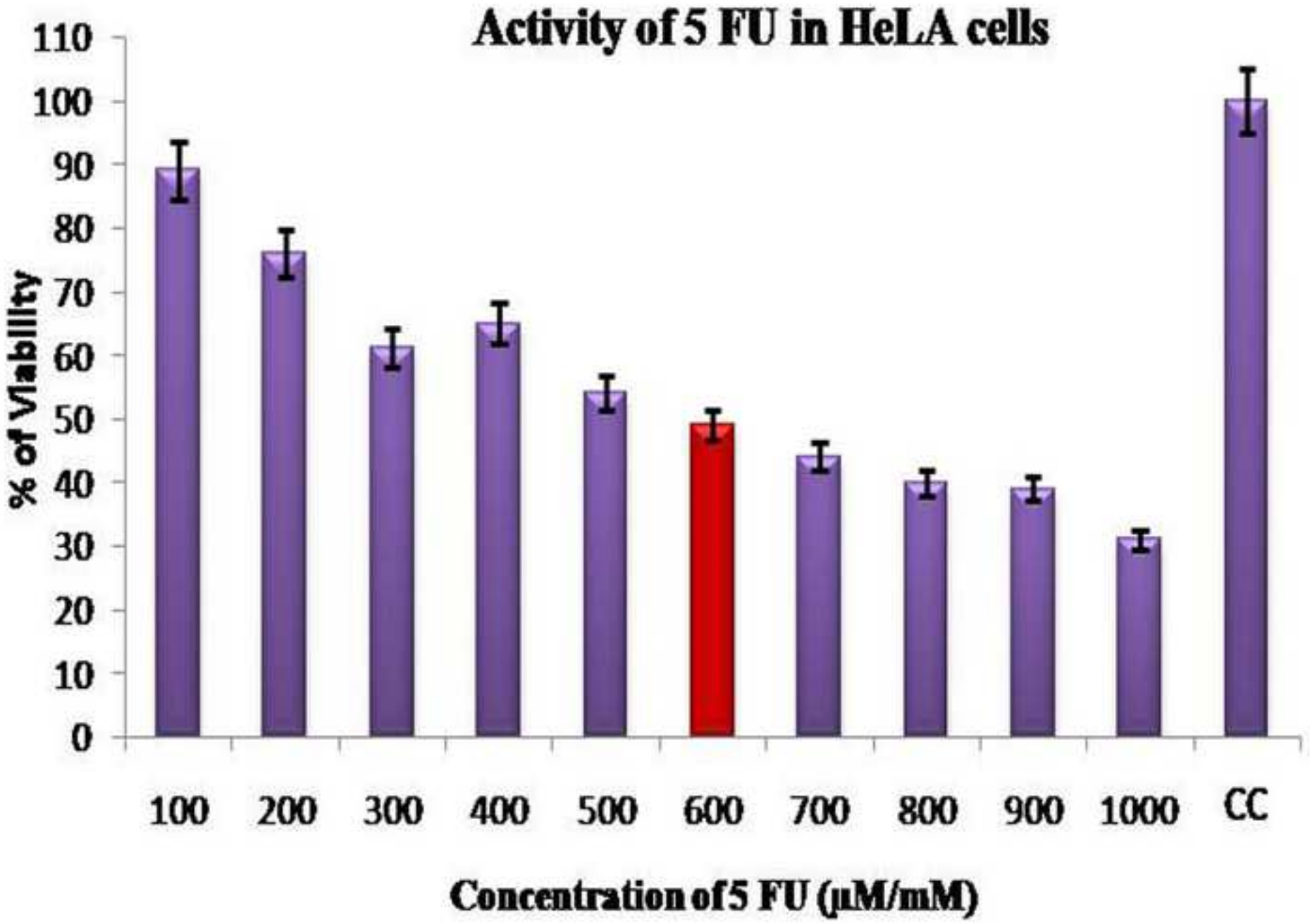

Fig 6c

Click here to download high resolution image

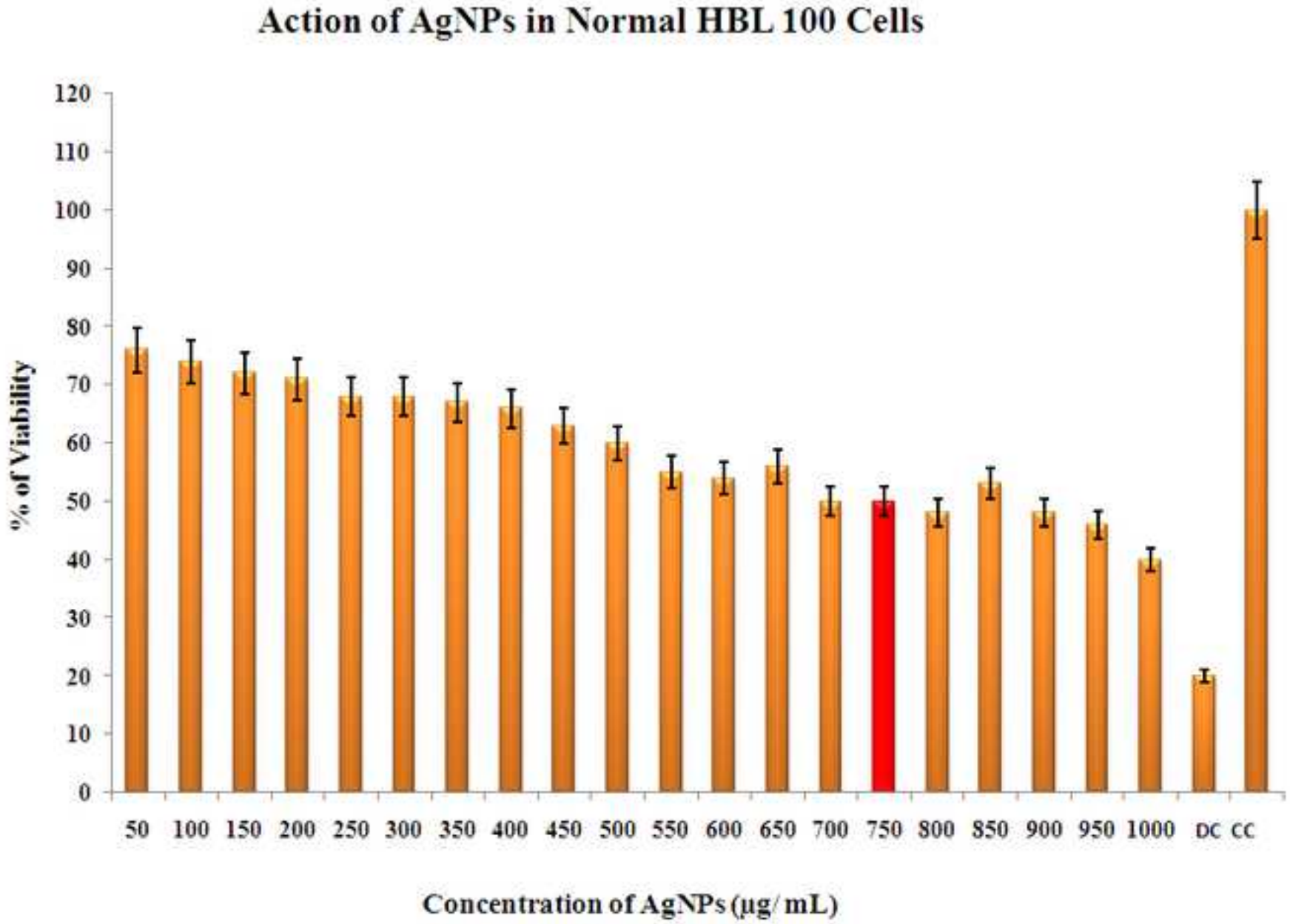

Fig 6d

Click here to download high resolution image

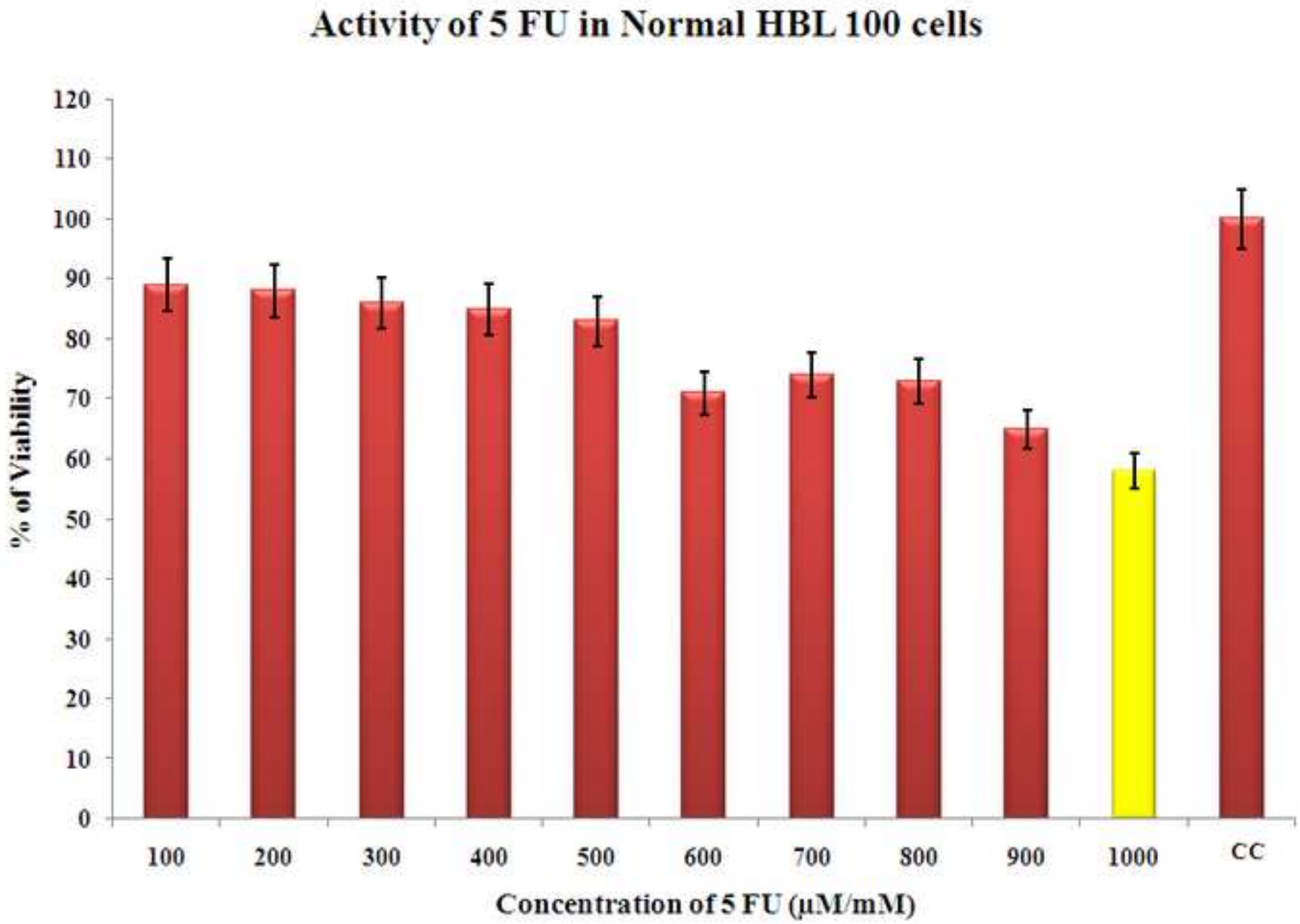

Fig. 7

Click here to download high resolution image

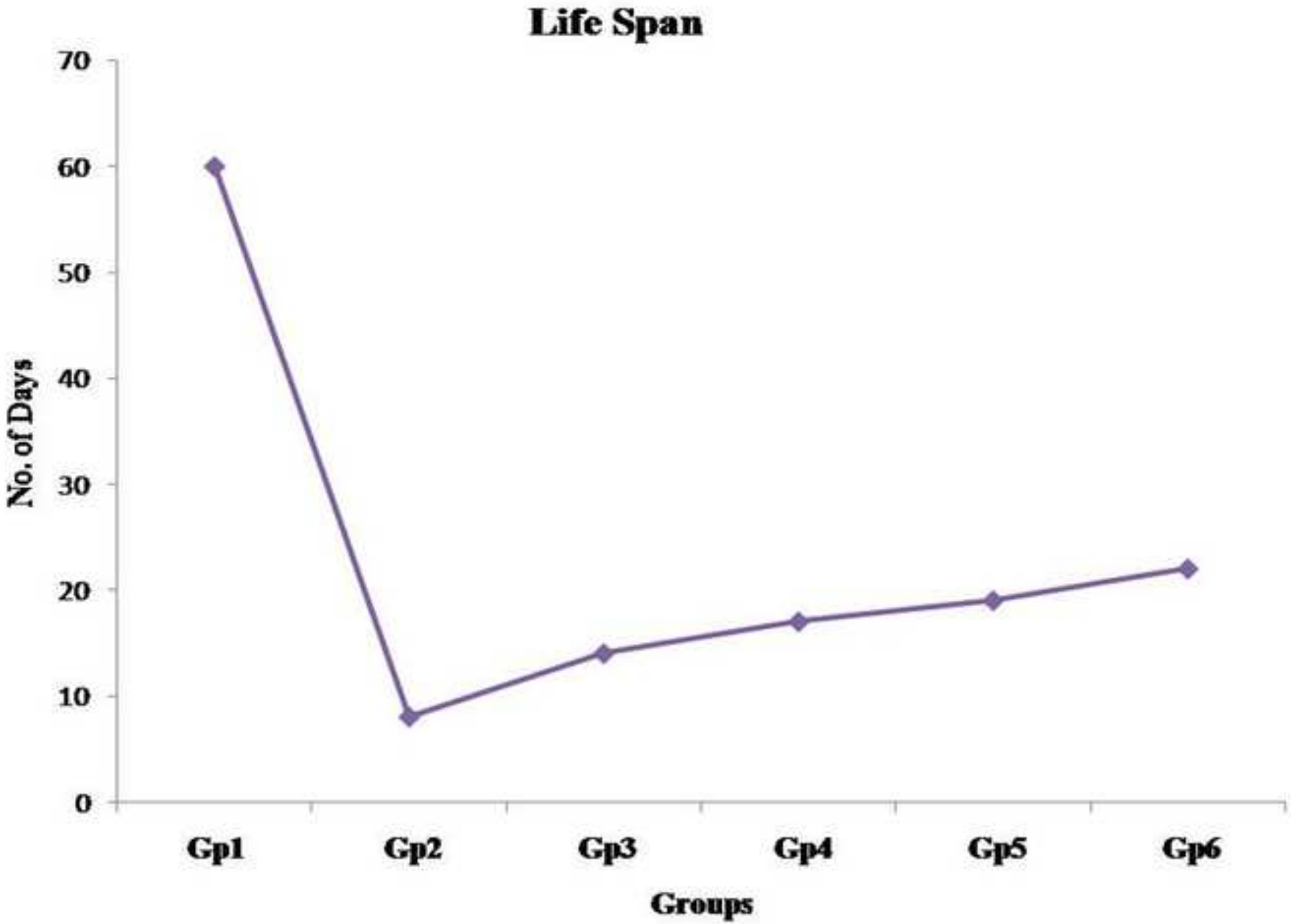

Fig. 8

Click here to download high resolution image